Gasoline aromatic: a critical determinant of urban secondary organic aerosol formation

Jianfei Peng[1,†], Min Hu[1, 4*], Zhuofei Du[1], Yinhui Wang[2], Jing Zheng[1], Wenbin Zhang[2], Yudong Yang[1], Yanhong Qin[1], Rong Zheng[2], Yao Xiao[1], Yusheng Wu[1], Sihua Lu[1], Zhijun Wu[1], Song Guo[1], Hongjun Mao[3], Shijin Shuai[2,*]

[1] State Key Joint Laboratory of Environmental Simulation and Pollution Control, College of Environmental Sciences and Engineering, Peking University, Beijing 100871, China
[2] State Key Laboratory of Automotive Safety and Energy, Tsinghua University, Beijing 100084, China
[3] College of Environmental Sciences and Engineering, Nankai University, Tianjin 300071, China
[4] Beijing Innovation Center for Engineering Science and Advanced Technology, Peking University
[†] Now at Department of Atmospheric Sciences, Texas A&M University, College Station, TX 77843, US

[*]Corresponding author: Min Hu, minhu@pku.edu.cn; Shijin Shuai, sjshuai@tsinghua.edu.cn

Abstract

Gasoline vehicle exhaust is an important contributor to secondary organic aerosol (SOA) formation in urban atmosphere. Fuel composition has potentially considerable impact on gasoline SOA production, but the link between fuel components and SOA production is still poorly understood. Here, we present chamber experiments to investigate the impacts of gasoline aromatic content on SOA production through chamber oxidation approach. A significant amplification factor of 3 - 6 for SOA productions from gasoline exhausts is observed as gasoline aromatic content rose from 29% to 37%. Considerably higher emission of aromatic volatile organic compounds (VOCs) using high-aromatic fuel plays an essential role in the SOA production enhancement, while the semi-VOCs (e.g., gas-phase PAHs) may also contribute to the higher SOA production. Our findings indicate that gasoline aromatics significantly influence ambient $PM_{2.5}$ concentration in urban area and highlight that more stringent regulation on gasoline aromatic content will achieve unexpected benefit on urban air quality.

1 Introduction

Fossil fuel-powered vehicles, an important source of NO_x, volatile organic compounds

(VOCs) and atmospheric particulate matter (PM), are always associated with the severe haze events, human health risks and climate forcing, particularly in urban areas (Parrish and Zhu, 2009; Guo et al., 2014; Huang et al., 2014; Kumar et al., 2014; Liu et al., 2015a; Kelly and Zhu, 2016; Peng et al., 2016b). Gasoline is the most widely used vehicle fuel and accounts for the largest total transportation energy consumptions in many countries, e.g., U.S. and China (NBSC, 2015; EIA, 2015). Among all the gasoline related PM components, secondary organic aerosols (SOA) produced via atmospheric oxidation of VOC precursors in the exhaust have been proved by chamber experiments as a large fraction, if not the largest, of gasoline vehicular PM (Zervas et al., 1999; Jimenez et al., 2009; Gordon et al., 2014a; Jathar et al., 2014; Platt et al., 2014; Liu et al., 2015b). Moreover, ambient measurement also demonstrated that gasoline SOA were the largest source of vehicular carbonaceous PM in megacities such as Los Angeles (Bahreini et al., 2012). However, although increasingly stringent gasoline fuel standards, especially on sulfur content, have been upgraded in the past decades in many countries to reduce the emissions, the impacts of fuel compositions on SOA production have not sufficiently been taken into account in the current gasoline fuel standards. This deficiency is mainly attributed to the poor understanding of the effects of fuel properties on the related SOA formation, and may ultimately lead to a policy bias on the control of vehicle emission regarding to the reduction of atmospheric pollution.

Aromatic hydrocarbons, unsaturated compounds with at least one benzene ring, account for 20% - 40% v/v of gasoline fuel. Aromatic VOCs (i.e., toluene, xylenes and trimethylbenzenes) react exclusively with the OH radical in the atmosphere, leading to the formation of a variety of semi- or low-volatile species (e.g., benzoic acid) (Zhang et al., 2015; Schwantes et al., 2017), which will partition onto existing particle and be recognized as anthropogenic SOA. Therefore, the higher emission of aromatic VOCs will likely result in more SOA formation potential. Existing fuel-effect experimental and model studies have shown that high-aromatic fuel in gasoline fuel will lead to more emissions of primary PM as well as some aromatic VOCs (Zervas et al., 1999; EPA, 2013; Karavalakis et al., 2015; Wang et al., 2016), indicating the considerable potential impact of gasoline aromatic content on SOA production. Furthermore, though aromatic content in diesel fuel may have insignificant impact on SOA formation (Gordon et al., 2014b), SOA production from gasoline vehicle is

considered more sensitive to aromatic content than that from diesel vehicle (Jathar et al., 2013). However, until now, very few studies have successfully quantified the impact of gasoline aromatic content on SOA production and directly revealed the possible pathway.

In this study, an in-depth comprehensive research was conducted to investigate the link between gasoline fuel compositions, primary gas- and particle- phase emission, and corresponding SOA formation. Gasoline exhaust emissions were examined on two platforms under two different conditions. The first platform was the chassis dynamometer system equipped with a constant volume sampler (CVS). Vehicle exhausts after CVS were introduced into an outdoor environmental chamber and subjected to aging under typical polluted urban conditions to simulate the SOA formation in ambient atmosphere. The second platform was the experimental engine system on which emissions from a port gasoline injection (PFI) engine and a gasoline direct injection (GDI) engine were examined. SOA formation experiments from engine exhausts were carried out with relatively high OH exposure compared to ambient conditions to obtain the SOA production potential. Most importantly, different gasoline fuels blended from different refinery streams were utilized in both platforms to probe the critical link among fuel components, VOCs emissions and related SOA production.

2 Materials and methods

2.1 Test fleet, cycle and engine.

A commercial PFI vehicle, an experimental PFI engine and a GDI engine were tested in this work.

The chosen PFI vehicle belonged to a commonly used vehicle model in China, which certified to China IV emission standard (equivalent to Euro 4). The mileage of the test fleet was about 3000 km. The fleet was driven on a chassis dynamometer system (Burke E. Porter Machinery Company) using cold-start Beijing cycle in order to better simulate the actual driving situation in Beijing. Beijing cycle was about 17 min long, with highest speed about 50 km h^{-1} (Fig. S1). The temperature and the absolute humidity in the dynamometer room were kept at 23.0 ± 1.0° C and 8.4 ± 0.9 g m^{-3}, respectively, for all vehicle experiments (Table S1).

Vehicle exhaust underwent the first stage of dilution with filtered ambient air using a

constant volume sampler (CVS) operated at 5.5 m^3 min^{-1} for all experiments. Approximately 5.3 L min^{-1} of diluted exhaust from the CVS was introduced into the 1.2 m^3 chamber to be further diluted with the clean air in the chamber (Fig. 1). The average dilution factor was approximately 20 in the CVS and was approximately 15 in the chamber. During the entire cycle, a light-duty gasoline vehicle emissions testing system (HORIBA, Ltd.) was used to measure the average and real-time concentration of THC, CO_2, CO and NO_x. Besides, a filter based sampler (AVL SPC 472) was used to sample primary particles from gasoline vehicles for chemical composition analysis.

The PFI and GDI engines were manufactured by a domestic Chinese automaker and equipped with turbocharger together with downsized displacement. The PFI engine used in this study was an experimental one with an old three-way catalyst (TWC), while the GDI engine was a commercial one designed for vehicles meeting the national IV emission standard. The operation mode of the PFI and GDI engine for chamber experiments was 2000 round per minute with 50% load. After the engine became stable at this operating mode, the exhaust were introduced into the chamber passing through a heater (150^{o}C) and a filter, with a flowrate of 5 L/min. During the injection, the engine exhaust steam was continuously introduced from the exhaust pipe into the chamber through a 1-meter-long tubing for 1 min. Particle number, mass and chemical composition, as well as VOCs in the exhaust were characterized at the same operating mode. Primary particles were sampled a filter based sampler (AVL SPC 472) and particulate chemical compositions, i.e., ions, EC, OC and polar and nonpolar organic species, were analyzed using ion chromatography, EC/OC analyzer (SUNSET Laboratory Inc.) and gas chromatography mass spectrometry (GC-MS) (Guo et al., 2013), respectively. Detail description of the engine experiments can be found in our previous study (Du et al., 2017) and all engine experiments used in this study are illustrated in Table S2.

2.2 Fuels

Three fuels (F1, F2 and F3) were utilized in this study to investigate the impacts of the gasoline fuel on SOA formation. A commercial Phase V gasoline (F1 fuel) with equivalent octane number of 93 was used as the base fuel. F1 fuel contains 29.8% aromatics and 4.1%

olefin content (Table S3).

F2 fuel was blended from 80% of F6 fuel and 20% of refinery catalytic stream. Octane (18.8%) and aromatic content (28.5%) in F2 fuel are very similar with that in F1 fuel, with the only difference to be the olefin content.

F3 fuel was blended from 80% of F2 fuel, 15–20% of refinery reformate stream with high aromatic content and very small amount of o-octane and n-heptane to keep the same octane level. Compared with F2 fuel, F3 fuel contained similar olefin content (15.4%) but higher aromatic content (36.7%) (Table S3), but both F2 and F3 fuels meet the Phase V gasoline standard. On the basis of the aromatic contents, the F2 and F3 fuel can be well representative of the fuel normally used in the year around 2010 and after 2013, respectively, in Chinese market such as Beijing and Shanghai. The mass fraction of molecular components in all three fuels used in this study can be found in Table S4.

2.3 Chamber Simulation

The quasi-atmospheric aerosol evolution study (QUALITY) chamber was utilized to quantify SOA formation from both gasoline engine exhaust and gasoline vehicle exhaust. The 1.2 m^3 two-layer chamber composed of an inner layer of 0.13 mm PFA Teflon and an outer rigid 5.6 mm thick acrylic shell (Cyro Industries Acrylite, OP-4). Both layers allowed for efficient transmission of sunlight in UV ranges (Peng et al., 2016b). Pre-experiments showed that wall loss decreased the particle number concentration by about 50% in about 3.5 hours. SO_2 and NO_x decreased to about 50% after 20 hours, while toluene and isoprene did not show obvious wall loss during a two-day experiment (Peng et al., 2017).

Prior to each experiment, the QUALITY chamber was covered with two layers of anti-UV cloth to shield the chamber from sunlight and flushed by zero air with a flowrate of 10 L min^{-1} for more than 15 hours to ensure a clean condition. In both vehicle and engine experiments, excess (1 ml, 30% v/v) H_2O_2 was also injected into the chamber via the makeup zero air as an extra hydroxyl radical (OH) source after adding the exhaust. Chamber experiments were normally conducted from noon to later afternoon, with inside temperature of 30 - 35 °C and relative humidity (RH) of 40 - 60%. A suite of high time resolution state-of-the-art aerosol instruments were utilized to measure the gas concentration and a

153 comprehensive set of particle properties throughout the experiments, including concentrations
154 of HONO, SO_2, NO_x, O_3, CO, CO_2 and several VOCs, the particle diameter, mass, chemical
155 composition (Fig. 1 and Table S5).

156 Particle number distributions were measured with a scanning mobility particle sizer
157 (SMPS) system, which was composed by one differential mobility analyzer (DMA, TSI, Inc.,
158 model 3081) and one condensation particle counter (CPC, TSI, Inc., model 3772). The mass
159 concentration and size distribution of particle chemical compositions, including organic
160 aerosol (OA), sulfate, nitrate, ammonium and chloride, were measured by a high-resolution
161 time-of-flight aerosol mass spectrometer (HR-ToF-AMS, Aerodyne Research, Inc.). The
162 evolution of several VOCs was measured continually by a proton transfer reaction mass
163 spectrometer (PTR-MS, Ionicon HSL experiments). Dedicated gas monitors, including the
164 SO2, NOx, CO, CO_2 and O3 monitors (Thermo Inc.), were utilized, and calibrated each
165 experiment day. VOCs in the chamber were also sampled by canisters every 1 hour during
166 vehicle experiments and analyzed by GC-MS/FID system (Wang et al., 2015).

167 Zero airflow was connected to the chamber over entire experiment to make up the
168 sampling volume by the instruments. To minimize the sampling volume by the instruments,
169 all instruments except SMPS were connected with several three-way valves, which were
170 successively switched between the ambient air and the chamber very 15 or 30 min.

171 **3 Results**

172 **3.1 Simulation of SOA formation from gasoline exhausts.** The temporal evolution of gas-
173 and particle- phase species during the chamber experiment is illustrated in Figure 2. The
174 initial concentration of NO_x, benzene and toluene in the chamber were 163 ppb, 5.6 ppb and
175 16.8 ppb, respectively, corresponding to the severe urban haze condition in the megacities
176 (Guo et al., 2014). After the chamber was exposed to the sunlight, 99% of NO was converted
177 to NO_2 within the first 10 min. This is because the fast photolysis of H_2O_2 produced large
178 amount of OH radical and further HO_2/RO_2 radicals inside the chamber, which reacted with
179 NO to form NO_2 (Seinfeld and Pandis, 2006). Then, the concentration of O_3 increased rapidly
180 to approximately 400 ppb after 1 h exposure, and gradually decreased later in this experiment
181 (Fig.2a).

182 Over the entire experiment, benzene and toluene experienced gentle decay in the

concentrations, but with different decay coefficients (Fig. 2b). Aerosol evolution is always characterized by a photochemical-age-based parameterization method in ambient measurements as well as chamber experiments (Hu et al., 2013; de Gouw et al., 2005; Peng et al., 2016a). Therefore, in order to compare our SOA productions in different experiments (in which solar flux were different), OH exposures were calculated based on the ratios of benzene and toluene concentrations, which reacted at different rates with OH radical (de Gouw et al., 2005). Besides, to compare the OH exposure in our chamber experiments with the previous ambient measurements, the OH concentration in the ambient air was assumed as 1.6×10^6 molec cm^{-3} (Hu et al., 2013; Peng et al., 2016a), and the equivalent photochemical ages of chamber experiments were then estimated by the ratio of OH exposure in the chamber to the assumed OH concentration in the ambient air.

New particle formation occurred inside the chamber within 10 min of exposure to the sunlight (Fig. 2c). These newly formed particles performed as seeds for the further formation of secondary species. A large quantity of secondary aerosols was then formed in the chamber, leading to the fast growth in the diameter of these particles to approximately 70 nm after 3h aging. The measurement of the particle compositions by the AMS reveals that the largest mass fraction of secondary aerosols in the chamber was SOA (approximately 95%, Fig. S2), indicating the critical role of the SOA for the secondary aerosol formation from gasoline exhausts. Because of the low aerosol loading (initially lower than 2 μg m^{-3}) and low relative humidity (40 - 50%) inside the chamber, heterogeneous reactions and aqueous phase processing were not important for the formation of SOA in this study (Zhang et al., 2015). Furthermore, the O:C ratio of SOA formed in the chamber stayed stable around 0.4 over the entire experiment, indicating that condensed phase reactions, i.e., aqueous or heterogeneous reactions, which produce highly oxidized oligomers, was not significant in the chamber experiments in this study. These SOA, therefore, were likely formed via condensation of less volatile products oxidized through gas phase reactions of VOCs precursors with limited multigenerational chemistry (Robinson et al., 2007; Jimenez et al., 2009; Jathar et al., 2014). The AMS spectrum profile of gasoline SOA obtained in this study was highly correlated with the ambient low oxidized secondary organic aerosols (LO-OOA) in Beijing (R^2=0.99, Fig. S3), further confirming the important contribution of gasoline emission on ambient $PM_{2.5}$.

SOA productions per fuel consumption or mileage were calculated on the basis of SOA mass concentration inside the chamber, dilution factors both in the CVS and inside the chamber, and fuel consumption/mileage of our working cycle. SOA mass concentration inside the chamber was corrected according to the particle wall loss curve (Fig. S4) as well as the dilution effect of both particles and gas precursors duo to the make-up zero air (Fig. S5). SOA production at the end of this experiment was calculated to be 80 mg kg-fuel^{-1}, or 6.7 mg km^{-1} after 3.5-hour aging (Fig. 2d). These values were 6.8 times higher than the emission factors (EFs) of primary particles (including both primary organic matters and elemental carbon) at the same cycle.

3.2 Fuel impacts on SOA production. The average fuel consumption per unit distance using F1, F2 and F3 fuels were 0.113, 0.112 and 0.113 L km^{-1}, respectively, indicating no difference in fuel economy among the three fuels. On the other hand, high-aromatic content gasoline led to noticeably large enhancement on SOA production from both vehicle and engine experiments. As illustrated in Figure 3a, the final SOA production from gasoline vehicle exhaust ranged from 30 mg kg-fuel^{-1} to 98 mg kg-fuel^{-1} at the end of each experiment, comparable to the results from cold start experiments in previous studies (Gordon et al., 2014a; Jathar et al., 2014). Experiments using F3 fuel (with 36.7 % v/v aromatic content) exhibit the highest SOA production factors, followed by F1 fuel (with 29.8 % v/v aromatics content) and F2 fuel (with 28.5 % v/v aromatics content), successively. The average SOA production at 12 equivalent photochemical-hours using F3 fuel was 76 mg kg-fuel^{-1} (6.3 mg km^{-1}), equivalent to 3 times of that using F2 fuel (25 mg kg-fuel^{-1}, 2.1 mg km^{-1}). Additionally, we observed much larger amount of the SOA formation in the first few photochemical hours in all experiments. The average production rates of SOA were as high as 5 - 13 mg kg^{-1} h^{-1} over each experiment, suggesting that the first-generation oxidation of some precursors inside the chamber produced large amount of SOA. This indicated the existence of some semi-volatile organic compounds (SVOCs) (Robinson et al., 2007; Keyte et al., 2013). It is worth to mention that as the concentrations of gas pollutants and formed SOA in the chamber using F3 fuel were 2-3 folders of those fusing F2 fuel, the partitioning of SVOCs in the experiments using F3 fuel might slightly benefit the SOA formation. This partitioning, however, would not qualitatively change the experiment conclusion that higher fuel aromatics

led to higher SOA production.

SOA formation experiments from the PFI engine exhaust were conducted under high oxidizing condition to obtain the SOA formation potential. As illustrated in Figure 3b, most of the SOA were formed within the first half an hour of each engine experiment and very little increase was observed over the following hours. The SOA formation potential from the engine exhaust using F3 fuel was 3.3 g kg-fuel^{-1} at this condition, equivalent to 5.8 times of that using F2 fuel, which was 0.57 g kg-fuel^{-1} on average. The high emission of the experimental PFI engine suggests that the results of engine experiments could represent the SOA production from gasoline vehicles with higher emission factor. Therefore, our results with two different experimental sets (vehicle and engine experiments) demonstrate the applicability of the SOA formation enhancement using high-aromatic fuel for gasoline vehicle with either high or low emission factor, at either representative cycle condition or steady-state operating condition.

Though good reproducibility was found for SOA production using either F2 or F3 fuels, there were inevitably several biases in the chamber simulation approach. For example, the SOA production in both vehicle and engine experiments might be underestimated due to loss of SVOC vapors to the chamber wall as well as the condensation of low organic vapor onto the particles that already lost on the chamber wall (Zhang et al., 2014). Also, the SOA production in engine experiments could be overestimated because the high concentration in the chamber might drive the gas-particle partitioning of the SVOCs into particle phase (Robinson et al., 2007). Nevertheless, the relative enhancement factor of SOA for different fuels was not largely influenced by these biases.

3.3 Aromatic emission and SOA production. To reveal the reason of this large amplification on SOA production owing to fuel constitution, gasoline PM and VOC emissions using F2 and F3 fuels were investigated (Fig. 4). Significant differences in the EFs among different gas- and particle-phase species were observed. For example, the EFs of primary PM in both number and mass concentration using F3 fuel were only 20% larger than those using F2 fuel, consistent with previous studies (EPA, 2013; Karavalakis et al., 2015). Similar results were also obtained for most of the alkane VOCs as well as NO. On the contrary, the EFs for SOA, aromatic VOCs and particle-phase Polycyclic Aromatic Hydrocarbons (PAHs)

exhibited marked enhancement using high-aromatic gasoline fuel. The EFs of each aromatic VOCs from the exhaust experiment increased by a factor of 0.2 - 9.5 using high-aromatic gasoline fuel, with enhancement factors of 3.3 and 2.7 for total aromatic VOCs in vehicle and engine experiments, respectively (Fig. 4). Coincidentally, the total particle-phase PAHs emission was amplified for 1.8 times using high-aromatic gasoline fuel (F3 vs F2), with the amplification factor of each PAH species varied from 1.1 to 2.2. Since both gas-phase aromatic VOCs (one ring) and particle-phase PAHs (mostly 3-7 rings) exhibited much higher EFs using high-aromatic gasoline fuel, it is reasonable to speculate higher EFs of the semi-volatile PAHs (2-3 rings) in our experiments.

Aromatic components in the exhaust mainly come from two routes, which are the survival of fuel aromatic contents and the combustion-derived formation in the engine. Ethylene and acetylene are the key species for the combustion-derived aromatics. High concentrations of ethylene and acetylene accelerate the acetylene addition reaction, which generates light aromatic VOC as well as PAHs in the engine (Wang and Frenklach, 1997; Frenklach, 2002). In this study, when the high-aromatic fuel was used, the concentrations of ethylene and acetylene from GDI engine were enhanced by a factor of 3.3 and 2.7, respectively, indicating that more aromatics were formed through the addition reaction of acetylene and ethylene in the engine.

SOA production ($\Delta OA_{predicted}$) from VOC precursors in the exhaust was roughly estimated by multiplying the mass loss of each VOC precursors (Δi) by its SOA yield, *Yi* (Donahue et al., 2006):

$$\Delta OA_{predicted} = \sum_i (\Delta_i \times Y_i) \quad (1)$$

The SOA precursors here included benzene, toluene, C8-aromatics, C9-aromatics and styrene, which were all measured by PTR-MS during each experiment. The contributions of the alkenes and alkanes (7-11 carbons) to SOA formation in our experiments were also estimated using Equ 1 based on the off-line GC-MS measurement. Results showed that the measured alkenes and alkanes (7-11 carbons) only accounted for approximately 4% of the total predicted SOA concentration (Fig. S6) duo to the low emission factors as well as the small

reacted proportion of these species inside the chamber. The yields of VOCi under high NOx condition are used (Ng et al., 2007; Platt et al., 2013), due to the low initial VOCs/NOx ratios which ranged from 0.5 to 1.0.

Figure 5 exhibits the two typical vehicle experiments with observed and predicted SOA concentration as a function of photochemical age using F2 and F3 fuels, respectively. The predicted SOA in the end of the two experiments accounted for 46% and 30% of the observed SOA formation with toluene and C9-aromatics to be the largest contributors, consistent with the previous results (Nordin et al., 2013; Platt et al., 2013; Gordon et al., 2014a). Predicted SOA concentration using F3 fuel was about 90% higher than that using F2 fuel, suggesting the import role of single-ring aromatic VOCs on the enhancement of SOA formation using high-aromatic fuel. However, more than 50 % of the SOA concentration cannot be explained by gas-phase oxidation of these single-ring aromatic VOCs. This value was even higher (up to 80%) in the first few photochemical hours in both experiments. Additionally, much larger percentage of SOA using F3 fuel cannot be explained by the single-ring aromatic VOCs. This suggests the existence of some unspeicated organic vapors, most likely SVOCs, which are considered to have high SOA yield and might partition to particle phase after the first-generation oxidation (Robinson et al., 2007; Chan et al., 2009; Jathar et al., 2014; Liu et al., 2015b). Two-ring and three-ring PAHs, e.g., naphthalene and phenanthrene, which were proved to have higher EFs using high-aromatic fuel (Chan et al., 2009), likely contributed importantly to the SVOC vapors and might play a crucial role for the enhancement of SOA production using high-aromatic fuel.

4 Discussion

Our results exhibit the critical impact of gasoline aromatics on urban SOA formation. We observed an amplification factor of 3-6 on SOA formation using high-aromatic gasoline, which was mainly caused by the high emission of one-ring aromatic VOCs as well as SVOC such as gas-phase PAHs. This enhancement of SOA formation, meanwhile, was found using not only a new vehicle meeting China IV emission standard, operated at a representative cycle condition in Beijing, but also an experimental engine which emitted more gaseous pollutants and was operated at steady state, suggesting the extensive applicability of our results.

Moreover, photo-oxidation of aromatics leads to significant production of small

dicarbonyls, i.e., glyoxal and methylglyoxal, which have high SOA yield via aqueous reactions (Zhang et al., 2015). If this aqueous SOA pathway is taken account, the influence of fuel on SOA formation will be much more remarkable. More work is needed to evaluate the aqueous pathway of SOA formation from gasoline exhaust.

Currently, aromatic content in gasoline fuel is increasing continuously in China, where more stringent standard on gasoline sulfur content has been upgraded and the oil refining procedure are changing to meet the new standard. For example, we found the average aromatic content for gasoline fuel in the market meeting Beijing Ⅲ, Ⅳ and Ⅴ standards were 23.4%, 28.5% and 36.3%, respectively. Recent study found that gasoline aromatic content in China was 9.6% higher than that in USA (Tang et al., 2015). Hence, the enhancement in SOA formation exerted by the increase of aromatic content in gasoline fuel from 29% to 37 % in this study can well represent the extra SOA formation due to the gasoline standard change in Beijing. Neglect of this side effect of fuel standard change may potentially offset the tremendous endeavors on vehicle emission control by the local government. From another perspective, our findings provide a new direction in controlling air pollution from vehicles, which is to decrease the aromatic content in the gasoline fuel. This may require more hydrogenation catalysis process in the petroleum refining procedure instead of catalytic reforming process, in which large amount of aromatic contents might be produced. Compared with the vehicle restriction regulation that met the shrill opposition voice from the society and the elimination of polluted vehicles that brought large amount of expenses, this direction might be more acceptable, efficient and economical. Additionally, current vehicle emission evaluation system, which mainly measures the emissions of PM, THC, NOx and CO, will fail to tell the consequences of using the high-aromatic gasoline fuel, as these species do not increase much when high-aromatic fuel is using (Fig. 4). Aromatic VOCs, especially the SVOC, should be considered in future vehicle emission evaluation.

Furthermore, this influence of gasoline aromatic content on air quality is not only adoptable in China. Strikingly, the current standard on gasoline aromatic content are not stringent enough in most of the countries and regions in the world, where fuel standards with very high maximum gasoline aromatic content (ranging from 35 % to 42% in different countries, Table S7) are implemented, even including some developed countries and regions,

i.e., Europe, Japan, Australia. Our findings highlight the necessity of a more stringent regulation on gasoline aromatic content in the next renewal of the gasoline standard.

Acknowledgement

This work was supported by the National Basic Research Program of China (973 Program) (2013CB228503, 2013CB228502, 2013CB955801); National Natural Science Foundation of China (91544214, 51636003, 41421064); the Strategic Priority Research Program of Chinese Academy of Sciences (XDB05010500); China Postdoctoral Science Foundation (2015M580929).

References

Bahreini, R., Middlebrook, A. M., de Gouw, J. A., Warneke, C., Trainer, M., Brock, C. A., Stark, H., Brown, S. S., Dube, W. P., Gilman, J. B., Hall, K., Holloway, J. S., Kuster, W. C., Perring, A. E., Prevot, A. S. H., Schwarz, J. P., Spackman, J. R., Szidat, S., Wagner, N. L., Weber, R. J., Zotter, P., and Parrish, D. D.: Gasoline emissions dominate over diesel in formation of secondary organic aerosol mass, Geophys. Res. Lett., 39, doi:10.1029/2011gl050718, 2012.

Chan, A. W. H., Kautzman, K. E., Chhabra, P. S., Surratt, J. D., Chan, M. N., Crounse, J. D., Kurten, A., Wennberg, P. O., Flagan, R. C., and Seinfeld, J. H.: Secondary organic aerosol formation from photooxidation of naphthalene and alkylnaphthalenes: implications for oxidation of intermediate volatility organic compounds (IVOCs), Atmos. Chem. Phys., 9, 3049-3060, doi:10.5194/acp-9-3049-2009, 2009.

de Gouw, J. A., Middlebrook, A. M., Warneke, C., Goldan, P. D., Kuster, W. C., Roberts, J. M., Fehsenfeld, F. C., Worsnop, D. R., Canagaratna, M. R., Pszenny, A. A. P., Keene, W. C., Marchewka, M., Bertman, S. B., and Bates, T. S.: Budget of organic carbon in a polluted atmosphere: Results from the New England Air Quality Study in 2002, J. Geophys. Res.-Atmos., 110, doi:10.1029/2004jd005623, 2005.

Donahue, N. M., Robinson, A. L., Stanier, C. O., and Pandis, S. N.: Coupled partitioning, dilution, and chemical aging of semivolatile organics, Environ. Sci. Technol., 40, 2635-2643, doi:10.1021/es052297c, 2006.

Du, Z., Hu, M., Peng, J., Guo, S., Zheng, R., Zheng, J., Shang, D., Qin, Y., Niu, H., Li, M.,

392 Yang, Y., Lu, S., Wu, Y., Shao, M., and Shuai, S.: The Potential of Secondary Aerosol
393 Formation from Chinese Gasoline Engine Exhaust. *J. Environ. Sci.*, in press, 2017.
394 Energy Information Administration U.S. (EIA): October 2014 Monthly Energy Review,
395 DOE/EIA-0035(2014/10), http://www.eia.gov/totalenergy/data/monthly/pdf/mer.pdf,
396 2014.
397 Environmental Protection Agency U.S. (EPA): Assessing the Effect of Five Gasoline
398 Properties on Exhaust Emissions from Light-Duty Vehicles Certified to Tier 2 Standards:
399 Analysis of Data from EPAct Phase 3., EPA-420-R-13-002:232-233, 2013.
400 Frenklach, M.: Reaction mechanism of soot formation in flames, Phys. Chem. Chem. Phys., 4,
401 2028-2037, doi:10.1039/b110045a, 2002.
402 Gordon, T. D., Presto, A. A., May, A. A., Nguyen, N. T., Lipsky, E. M., Donahue, N. M.,
403 Gutierrez, A., Zhang, M., Maddox, C., Rieger, P., Chattopadhyay, S., Maldonado, H.,
404 Maricq, M. M., and Robinson, A. L.: Secondary organic aerosol formation exceeds
405 primary particulate matter emissions for light-duty gasoline vehicles, Atmos. Chem. and
406 Phys., 14, 4661-4678, doi:10.5194/acp-14-4661-2014, 2014a.
407 Gordon, T. D., Presto, A. A., Nguyen, N. T., Robertson, W. H., Na, K., Sahay, K. N., Zhang,
408 M., Maddox, C., Rieger, P., Chattopadhyay, S., Maldonado, H., Maricq, M. M., and
409 Robinson, A. L.: Secondary organic aerosol production from diesel vehicle exhaust:
410 impact of aftertreatment, fuel chemistry and driving cycle, Atmos. Chem. Phys., 14,
411 4643-4659, doi:10.5194/acp-14-4643-2014, 2014b.
412 Guo, S., Hu, M., Guo, Q., Zhang, X., Schauer, J. J., and Zhang, R.: Quantitative evaluation of
413 emission controls on primary and secondary organic aerosol sources during Beijing 2008
414 Olympics, Atmos. Chem. Phys., 13, 8303-8314, 2013.
415 Guo, S., Hu, M., Zamora, M. L., Peng, J. F., Shang, D. J., Zheng, J., Du, Z. F., Wu, Z., Shao,
416 M., Zeng, L. M., Molina, M. J., and Zhang, R. Y.: Elucidating severe urban haze
417 formation in China, P. Natl. Acad. Sci. U.S.A., 111, 17373-17378,
418 doi:10.1073/pnas.1419604111, 2014.
419 Hu, W. W., Hu, M., Yuan, B., Jimenez, J. L., Tang, Q., Peng, J. F., Hu, W., Shao, M., Wang,
420 M., Zeng, L. M., Wu, Y. S., Gong, Z. H., Huang, X. F., and He, L. Y.: Insights on organic
421 aerosol aging and the influence of coal combustion at a regional receptor site of central

eastern China, Atmos. Chem. Phys., 13, 10095-10112, doi:10.5194/acp-13-10095-2013, 2013.

Huang, R.-J., Zhang, Y., Bozzetti, C., Ho, K.-F., Cao, J.-J., Han, Y., Daellenbach, K. R., Slowik, J. G., Platt, S. M., Canonaco, F., Zotter, P., Wolf, R., Pieber, S. M., Bruns, E. A., Crippa, M., Ciarelli, G., Piazzalunga, A., Schwikowski, M., Abbaszade, G., Schnelle-Kreis, J., Zimmermann, R., An, Z., Szidat, S., Baltensperger, U., Haddad, I. E., and Prévôt, A. S. H.: High secondary aerosol contribution to particulate pollution during haze events in China, Nature, doi:10.1038/nature13774, 2014.

Jathar, S. H., Miracolo, M. A., Tkacik, D. S., Donahue, N. M., Adams, P. J., and Robinson, A. L.: Secondary Organic Aerosol Formation from Photo-Oxidation of Unburned Fuel: Experimental Results and Implications for Aerosol Formation from Combustion Emissions, Environ. Sci. Technol., 47, 12886-12893, doi:10.1021/es403445q, 2013.

Jathar, S. H., Gordon, T. D., Hennigan, C. J., Pye, H. O., Pouliot, G., Adams, P. J., Donahue, N. M., and Robinson, A. L.: Unspeciated organic emissions from combustion sources and their influence on the secondary organic aerosol budget in the United States, P. Natl. Acad. Sci. U.S.A., 111, 10473-10478, doi:10.1073/pnas.1323740111, 2014.

Jimenez, J. L., Canagaratna, M. R., Donahue, N. M., Prevot, A. S. H., Zhang, Q., Kroll, J. H., DeCarlo, P. F., Allan, J. D., Coe, H., Ng, N. L., Aiken, A. C., Docherty, K. S., Ulbrich, I. M., Grieshop, A. P., Robinson, A. L., Duplissy, J., Smith, J. D., Wilson, K. R., Lanz, V. A., Hueglin, C., Sun, Y. L., Tian, J., Laaksonen, A., Raatikainen, T., Rautiainen, J., Vaattovaara, P., Ehn, M., Kulmala, M., Tomlinson, J. M., Collins, D. R., Cubison, M. J., Dunlea, J., Huffman, J. A., Onasch, T. B., Alfarra, M. R., Williams, P. I., Bower, K., Kondo, Y., Schneider, J., Drewnick, F., Borrmann, S., Weimer, S., Demerjian, K., Salcedo, D., Cottrell, L., Griffin, R., Takami, A., Miyoshi, T., Hatakeyama, S., Shimono, A., Sun, J. Y., Zhang, Y. M., Dzepina, K., Kimmel, J. R., Sueper, D., Jayne, J. T., Herndon, S. C., Trimborn, A. M., Williams, L. R., Wood, E. C., Middlebrook, A. M., Kolb, C. E., Baltensperger, U., and Worsnop, D. R.: Evolution of Organic Aerosols in the Atmosphere, Science, 326, 1525-1529, doi:10.1126/science.1180353, 2009.

Karavalakis, G., Short, D., Vu, D., Russell, R., Hajbabaei, M., Asa-Awuku, A., and Durbin, T. D.: Evaluating the Effects of Aromatics Content in Gasoline on Gaseous and Particulate

452 Matter Emissions from SI-PFI and SIDI Vehicles, Environ. Sci. Technol., 49, 7021-7031,
453 doi:10.1021/es5061726, 2015.
454 Kelly, F. J., and Zhu, T.: Transport solutions for cleaner air, Science, 352, 934-936,
455 doi:10.1126/science.aaf3420, 2016.
456 Keyte, I. J., Harrison, R. M., and Lammel, G.: Chemical reactivity and long-range transport
457 potential of polycyclic aromatic hydrocarbons - a review, Chem Soc Rev, 42, 9333-9391,
458 10.1039/c3cs60147a, 2013.
459 Kumar, P., Morawska, L., Birmili, W., Paasonen, P., Hu, M., Kulmala, M., Harrison, R. M.,
460 Norford, L., and Britter, R.: Ultrafine particles in cities, Environ. Int., 66, 1-10,
461 doi:10.1016/j.envint2014.01.013, 2014.
462 Liu, S., Aiken, A. C., Gorkowski, K., Dubey, M. K., Cappa, C. D., Williams, L. R., Herndon,
463 S. C., Massoli, P., Fortner, E. C., Chhabra, P. S., Brooks, W. A., Onasch, T. B., Jayne, J.
464 T., Worsnop, D. R., China, S., Sharma, N., Mazzoleni, C., Xu, L., Ng, N. L., Liu, D.,
465 Allan, J. D., Lee, J. D., Fleming, Z. L., Mohr, C., Zotter, P., Szidat, S., and Prevot, A. S.
466 H.: Enhanced light absorption by mixed source black and brown carbon particles in UK
467 winter, Nat. Commun., 6, doi:10.1038/Ncomms9435, 2015a.
468 Liu, T., Wang, X., Deng, W., Hu, Q., Ding, X., Zhang, Y., He, Q., Zhang, Z., Lu, S., Bi, X.,
469 Chen, J., and Yu, J.: Secondary organic aerosol formation from photochemical aging of
470 light-duty gasoline vehicle exhausts in a smog chamber, Atmos. Chem. Phys., 15,
471 9049-9062, doi:10.5194/acp-15-9049-2015, 2015b.
472 NBSC National Bureau of Statistics of China: China Statistical Yearbook, China Statistics
473 Press, 2015.
474 Ng, N. L., Kroll, J. H., Chan, A. W. H., Chhabra, P. S., Flagan, R. C., and Seinfeld, J. H.:
475 Secondary organic aerosol formation from m-xylene, toluene, and benzene, Atmos. Chem.
476 Phys., 7, 3909-3922, 2007.
477 Nordin, E. Z., Eriksson, A. C., Roldin, P., Nilsson, P. T., Carlsson, J. E., Kajos, M. K., Hellén,
478 H., Wittbom, C., Rissler, J., Löndahl, J., Swietlicki, E., Svenningsson, B., Bohgard, M.,
479 Kulmala, M., Hallquist, M., and Pagels, J. H.: Secondary organic aerosol formation from
480 idling gasoline passenger vehicle emissions investigated in a smog chamber, Atmos.
481 Chem. Phys., 13, 6101-6116, doi:10.5194/acp-13-6101-2013, 2013.

Parrish, D. D., and Zhu, T.: Clean Air for Megacities, Science, 326, 674-675, doi:10.1126/science.1176064, 2009.

Peng, J. F., Hu, M., Gong, Z. H., Tian, X. D., Wang, M., Zheng, J., Guo, Q. F., Cao, W., Lv, W., Hu, W. W., Wu, Z. J., and Guo, S.: Evolution of secondary inorganic and organic aerosols during transport: A case study at a regional receptor site, Environ. Pollut., 218, 794-803, doi:10.1016/j.envpol.2016.08.003, 2016a.

Peng, J. F., Hu, M., Guo, S., Du, Z. F., Zheng, J., Shang, D. J., Zamora, M. L., Zeng, L. M., Shao, M., Wu, Y. S., Zheng, J., Wang, Y., Glen, C. R., Collins, D. R., Molina, M. J., and Zhang, R. Y.: Markedly enhanced absorption and direct radiative forcing of black carbon under polluted urban environments, P. Natl. Acad. Sci. U.S.A., 113, 4266-4271, doi:10.1073/pnas.1602310113, 2016b.

Peng, J., Hu, M., Guo, S., Du, Z., Shang, D., Zheng, J., Zheng, J., Zeng, L., Shao, M., Wu, Y., Colllins, D., and Zhang, R.: Aging and hygroscopicity variation of black carbon particles in Beijing measured by a quasi-atmospheric aerosol evolution study (QUALITY) chamber, Atmos. Chem. Phys. Discuss., https://doi.org/10.5194/acp-2017-370, in review, 2017.

Platt, S. M., El Haddad, I., Zardini, A. A., Clairotte, M., Astorga, C., Wolf, R., Slowik, J. G., Temime-Roussel, B., Marchand, N., Ježek, I., Drinovec, L., Močnik, G., Möhler, O., Richter, R., Barmet, P., Bianchi, F., Baltensperger, U., and Prévôt, A. S. H.: Secondary organic aerosol formation from gasoline vehicle emissions in a new mobile environmental reaction chamber, Atmos. Chem. Phys., 13, 9141-9158, doi:10.5194/acp-13-9141-2013, 2013.

Platt, S. M., El Haddad, I., Pieber, S. M., Huang, R. J., Zardini, A. A., Clairotte, M., Suarez-Bertoa, R., Barmet, P., Pfaffenberger, L., Wolf, R., Slowik, J. G., Fuller, S. J., Kalberer, M., Chirico, R., Dommen, J., Astorga, C., Zimmermann, R., Marchand, N., Hellebust, S., Temime-Roussel, B., Baltensperger, U., and Prevot, A. S. H.: Two-stroke scooters are a dominant source of air pollution in many cities, Nat. Commun., 5, doi:10.1038/Ncomms4749, 2014.

Robinson, A. L., Donahue, N. M., Shrivastava, M. K., Weitkamp, E. A., Sage, A. M., Grieshop, A. P., Lane, T. E., Pierce, J. R., and Pandis, S. N.: Rethinking Organic Aerosols: Semivolatile Emissions and Photochemical Aging, Science, 315, 1259-1262,

512 doi:10.1126/science.1133061, 2007.
513 Schwantes, R. H., Schilling, K. A., McVay, R. C., Lignell, H., Coggon, M. M., Zhang, X.,
514 Wennberg, P. O., and Seinfeld, J. H.: Formation of highly oxygenated low-volatility
515 products from cresol oxidation, Atmos. Chem. Phys., 17, 3453-3474, 2017.
516 Seinfeld, J.H., and Pandis, S.N.: Atmospheric Chemistry and Physics: From Air Pollution to
517 Climate Change, second ed. J. Wiley, New York, 2006.
518 Tang, G., Sun, J., Wu, F., Sun,Y., Zhu, X., Geng, Y. and Wang, Y.: Organic composition of
519 gasoline and its potential effects on air pollution in North China. Sci. China Chem. 58(9),
520 doi: 10.1007/s11426-015-5464-0, 2015.
521 Wang, H., and Frenklach, M.: A detailed kinetic modeling study of aromatics formation in
522 laminar premixed acetylene and ethylene flames, Combust. Flame, 110, 173-221,
523 doi:10.1016/S0010-2180(97)00068-0, 1997.
524 Wang, M., Shao, M., Chen, W., Lu, S., Liu, Y., Yuan, B., Zhang, Q., Zhang, Q., Chang, C. C.,
525 Wang, B., Zeng, L., Hu, M., Yang, Y., and Li, Y.: Trends of non-methane hydrocarbons
526 (NMHC) emissions in Beijing during 2002-2013, Atmos. Chem. Phys., 15, 1489-1502,
527 2015.
528 Wang Y., Zheng, R., Qin, Y., Peng, J., Li, M., Xing, J., Wu, Y., Hu, M., and Shuai S..: The
529 impact of fuel compositions on the particulate emissions of direct injection gasoline
530 engine, Fuel, 166, 543-552, doi:10.1016/j.fuel.2015.11.019, 2016.
531 Yuan, B., Hu, W. W., Shao, M., Wang, M., Chen, W. T., Lu, S. H., Zeng, L. M., and Hu, M.:
532 VOC emissions, evolutions and contributions to SOA formation at a receptor site in
533 eastern China, Atmos. Chem. Phys., 13, 8815-8832, doi:10.5194/acp-13-8815-2013, 2013.
534 Zervas, E., Montagne, X., and Lahaye, J.: The influence of gasoline formulation on specific
535 pollutant emissions, J. Air Waste. Manage., 49, 1304-1314, 1999.
536 Zhang, R., Wang, G., Guo, S., Zamora, M. L., Ying, Q., Lin, Y., Wang, W., Hu, M., and
537 Wang, Y.: Formation of urban fine particulate matter, Chem. Rev., 115, 3803-3855,
538 doi:10.1021/acs.chemrev.5b00067, 2015.
539 Zhang, X., Cappa, C. D., Jathar, S. H., Mcvay, R. C., Ensberg, J. J., Kleeman, M. J., and
540 Seinfeld, J. H.: Influence of vapor wall loss in laboratory chambers on yields of secondary
541 organic aerosol, P. Natl. Acad. Sci. U.S.A., 111, 5802-5807,

542 doi:10.1073/pnas.1404727111, 2014.

543

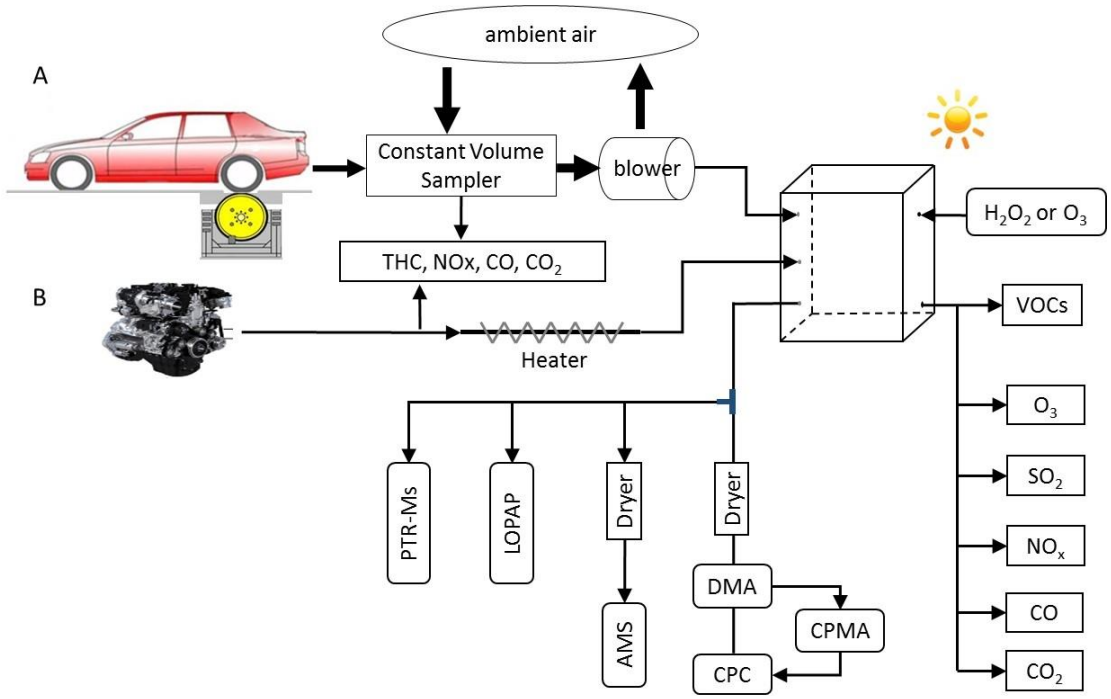

544

545 **Figure 1.** Schematic diagram of chamber experiments.

546

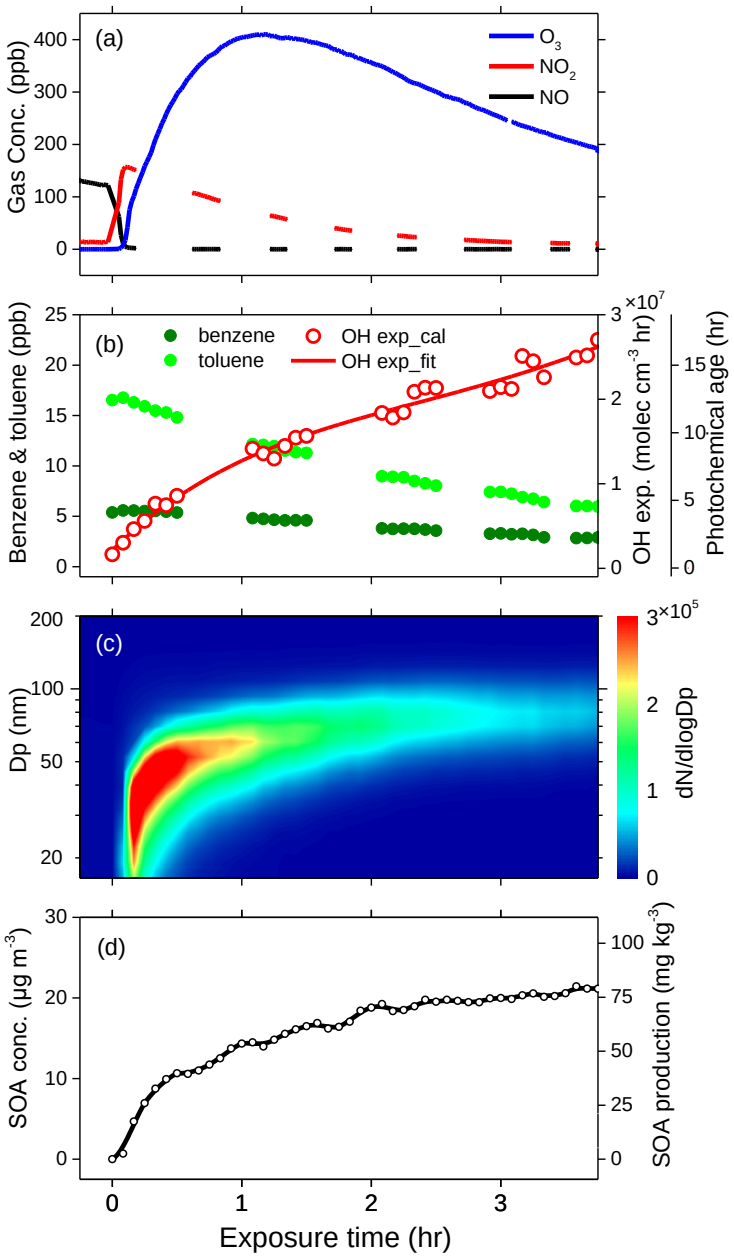

Figure 2. Evolution of gas-phase species (a, b), particle size distribution (c), and SOA concentration and production (d) during a typical chamber experiment (V2). OH exposure and photochemical age are calculated based on the ratios of benzene and toluene concentrations, assuming that OH concentration is 1.6 $\times 10^6$ molec cm^{-3}. The SOA mass concentration is obtained by intergrading size distribution of particles inside the chamber on the basis of measured particle density. The measured SOA mass concentration is corrected according to the particle wall loss curve as well as the dilution effect for both particles and gas precursors.

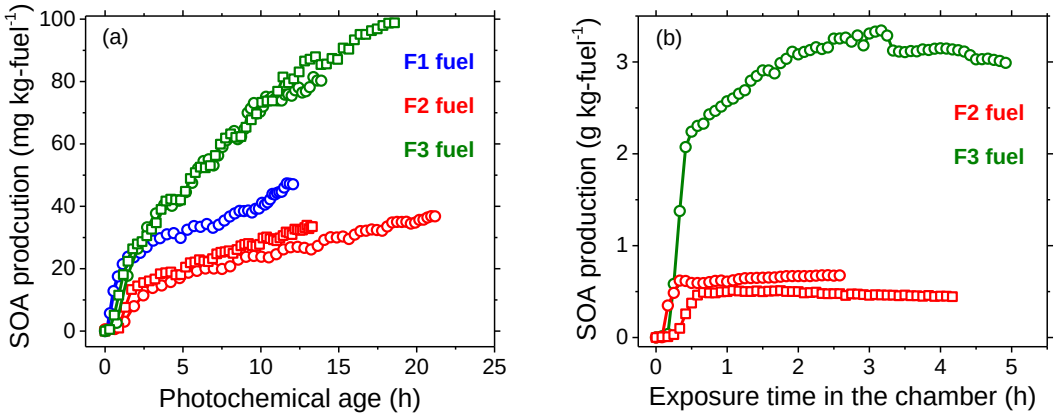

Figure 3. SOA production in the vehicle experiments as a function of photochemical age (a) and in the engine exhaust experiments as a function of exposure time (b). The green squares, green circles, red squares, red circles and blue circles (a) represent the experiment V1, V2, V3, V4 and V5 shown in Table S1, respectively. The green circles, red squares and red circles (b) represent the experiments E1, E2 and E3 shown in Table S2, respectively.

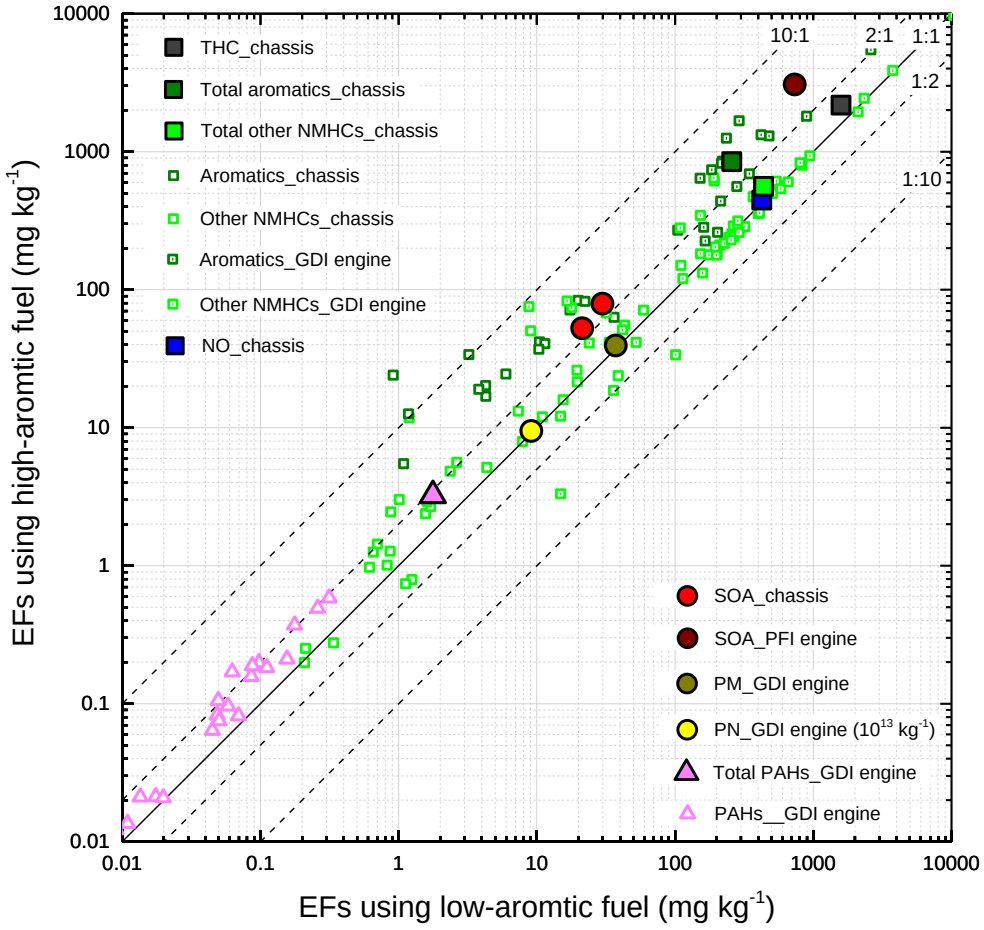

Figure 4. Comparison of emission factors (EFs) of gas- and particle species using high-aromatic fuel (F3 fuel) to those using low-aromatic fuel (F2 fuel). The total hydrocarbons (THC) were measured by vehicle emissions testing system, HORIBA, Ltd.), and the total aromatics and non-methane hydrocarbons (NMHCs) were measured by offline GC-MS. The black line denotes that the ratio of EFs using aromatic-rich fuel over aromatic-poor fuel is 1:1, and dashed lines stand for the ratios of 10:1, 2:1, 1:2, and 1:10, respectively. Note that the PAHs and VOCs data for the GDI engine were measured before the three-way Catalyst (TWC). Value in the figure can be found in Table S6.

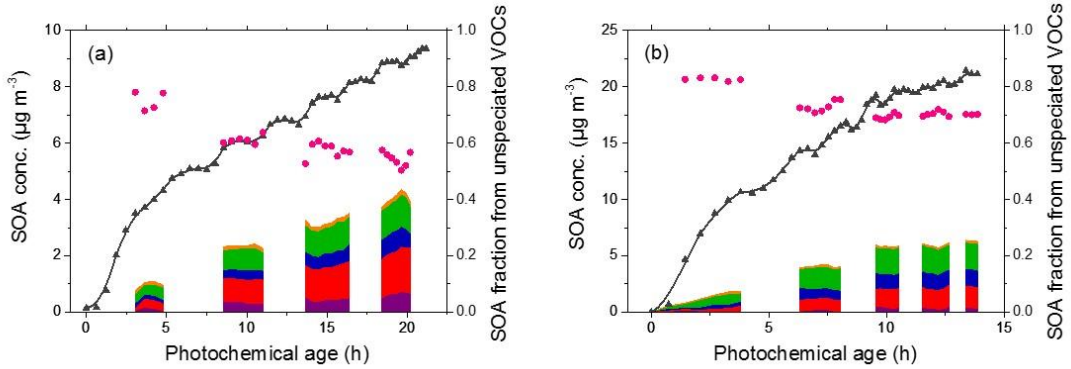

574

575 **Figure 5.** Observed and predicted SOA concentration, and SOA fraction from unspeciated
576 VOCs as a function of photochemical age in typical chamber experiments using (a) F2
577 (experiment V4) and (b) F3 (experiment V2) fuels. Black line and triangles represent the
578 corrected SOA concentrations in the chamber experiments. The purple, red, blue, green and
579 yellow areas represent the predicted SOA from the oxidation of benzene, toluene,
580 C8-aromatics, C9-aromatics and styrene, respectively. The pink circles represent the SOA
581 fractions that cannot predicted by the one-ring aromatic VOC precursors.

582

583